Study of orientation effect on nanoscale polarization in $BaTiO_3$ thin films using piezoresponse force microscopy

Il-Doo Kim, Ytshak Avrahami, and Harry L. Tuller
Department of Materials Science and Engineering, Massachusetts Institute of Technology, Cambridge, Massachusetts 02139

Young-Bae Park,[a] Matthew J. Dicken, and Harry A. Atwater
Thomas J. Watson Laboratories of Applied Physics, California Institute of Technology, Pasadena, California 91125

(Received 20 December 2004; accepted 16 March 2005; published online 3 May 2005)

We have investigated the effect of texture on in-plane (IPP) and out-of plane (OPP) polarizations of pulsed-laser-deposited $BaTiO_3$ thin films grown on Pt and $La_{0.5}Sr_{0.5}CoO_3$ (LSCO) buffered Pt electrodes. The OPP and IPP polarizations were observed by piezoresponse force microscopy (PFM) for three-dimensional polarization analyses in conjunction with conventional diffraction methods using x-ray diffraction and reflection high energy electron diffraction measurements. $BaTiO_3$ films grown on Pt electrodes exhibited highly (101) preferred orientation with higher IPP component whereas $BaTiO_3$ film grown on LSCO/Pt electrodes showed (001) and (101) orientations with higher OPP component. Measured effective d_{33} values of $BaTiO_3$ films deposited on Pt and LSCO/Pt electrodes were 14.3 and 54.0 pm/V, respectively. Local piezoelectric strain loops obtained by OPP and IPP-PFM showed that piezoelectric properties were strongly related to film orientation. © *2005 American Institute of Physics*. [DOI: 10.1063/1.1923173]

Extensive studies are being carried out on ferroelectric thin films, particularly those based on the barium titanate ($BaTiO_3$) system, for their application in electro-optic and electromechanical devices.[1–3] Barium titanate's large electro-optic coefficient, for example, can enable the fabrication of highly miniaturized optical modulators for fiber optic based data transmission systems.[4,5] Also, the large piezoelectric constants and electromechanical coupling coefficients are extremely attractive for a variety of sensor and actuator applications. The electro-optic and electromechanical properties are strongly related to crystallographic orientation, crystal phase, domain configuration, and substrate-imposed mechanical strain.[6,7] Few articles have reported on the effect of orientation on the nanolevel scale piezoelectric properties of polycrystalline $BaTiO_3$ thin films.

Recently, atomic force microscopy (AFM) in piezoresponse mode, also called piezoelectric force microscopy (PFM), has successfully demonstrated the capability of imaging ferroelectric domains and characterizing ferroelectric surfaces on nanometer levels.[8–10] In PFM measurements, the piezoelectric response, under voltage modulation, is detected as a vibration of the PFM cantilever with a conducting tip in direct contact with the surface of the film. These vibrations arise due to the converse piezoelectric effect and hence depend on the orientation of the polarization vector. The amplitude of the acquired signal is proportional to the effective longitudinal piezoelectric coefficient, d_{33}. In order to optimize the electromechanical performance of ferroelectric thin films, it is very important to understand the orientation dependence of the piezoelectric constants.

In this letter, we report the results of an investigation of the effect of film orientation of $BaTiO_3$ thin films grown on Pt and LSCO/Pt electrodes on piezoelectric properties by examining local piezoresponse hysteresis loops of nanometer-scale regions with the aid of piezoresponse force microscopy.

Disk-type $La_{0.5}Sr_{0.5}CoO_3$ (LSCO) and $BaTiO_3$ (BTO) targets were prepared by mixing the appropriate ratio of precursor oxide powders, pressing the powders into pellets, and sintering them to high density. Pulsed laser deposition (PLD) was carried out at a laser fluence of 2.0 J/cm^2 and a repetition rate of 25 Hz using a KrF excimer source ($\lambda = 248$ nm). $BaTiO_3$ thin films of 150–250 nm thick were grown onto the $Pt/Ta/SiO_2/Si$ and $LSCO/Pt/Ta/SiO_2/Si$ substrates. The substrate temperature and oxygen ambient pressure during PLD growth were 700 °C and 30 mTorr, respectively. The LSCO buffer layer (100 nm) was deposited onto the $Pt/Ta/SiO_2/Si$ substrate at 600 °C by PLD. X-ray diffraction (XRD: Rigaku, D/MAX-RC) and reflected high electron energy diffraction (RHEED) analyses were used to identify the phases and determine the preferred growth orientation. Contact mode-AFM (Autoprobe CP-R, Veeco) was used to image surface morphology and root-mean-square (rms) roughness. At the same time, PFM, with out-of plane and in-plane polarization (OPP/IPP) measurements which are proportional to the three orthogonal components (P_x, P_y, and P_z), allows the measurement of the local converse piezoelectric displacement and lateral torsion of the tip, respectively. The piezoelectric response signals from tip deflection (out-of plane polarization vector component) and lateral tip torsion (in-plane polarization vector component) were simultaneously obtained by PFM and lock-in amplifier techniques. PFM was performed using Co-coated silicon (*n* dope) cantilevers of triangular geometry which were modulated with an ac voltage of 1.5 V, resonance frequency of 1–2 kHz, and scan rate of 0.3 Hz.

Figure 1 shows the XRD patterns of 250 nm $BaTiO_3$ films grown on $Pt/Ta/SiO_2/Si$ and $LSCO/Pt/Ta/SiO_2/Si$ substrates, respectively. The $BaTiO_3$ film on $Pt/Ta/SiO_2/Si$ showed polycrystalline perovskite morphology with highly

[a]Electronic mail: ypark@caltech.edu

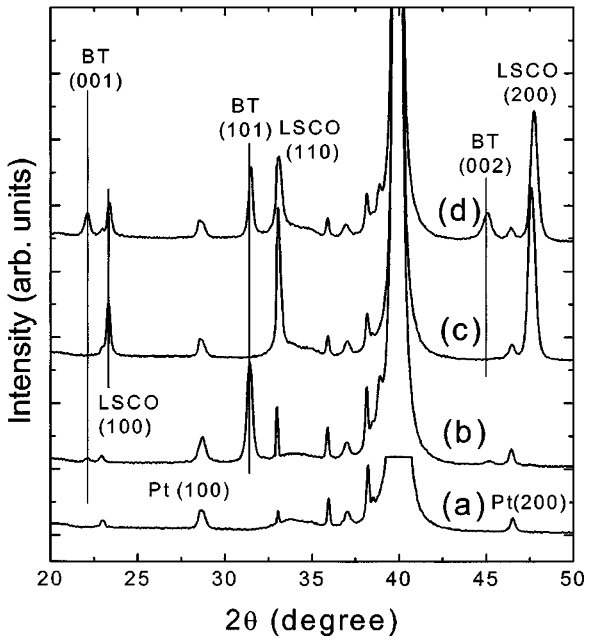

FIG. 1. XRD patterns of substrates and $BaTiO_3$ thin films. (a) $Pt/Ta/SiO_2/Si$, (b) $BaTiO_3/Pt/Ta/SiO_2/Si$, (c) $LSCO/Pt/Ta/SiO_2/Si$, and (d) $BaTiO_3/LSCO/Pt/Ta/SiO_2/Si$. Thickness of $BaTiO_3$ films is 250 nm.

(101) preferred orientation. In contrast the $BaTiO_3$ film deposited on 100 nm LSCO buffered $Pt/Ta/SiO_2/Si$ had mixed (001) and (101) orientation. The degree of (001) preferred orientation increased by using a LSCO buffer layer. X-ray diffraction also revealed that the LSCO films were single phase crystalline as shown in Fig. 1(c). LSCO has a pseudocubic perovskite structure with a lattice constant of 3.835 Å. The (001) preferred orientation is promoted as a consequence of the structural match between LSCO and $BaTiO_3$. In order to confirm the surface structure, RHEED measurements were performed on $BaTiO_3$ films grown on Pt and LSCO/Pt electrodes in an ultrahigh vacuum molecular beam epitaxy (UHV-MBE) chamber. RHEED patterns in Fig. 2 showed that both $BaTiO_3$ films had ring patterns, indicative of a polycrystalline phase with random orientation. However, an intense discontinuous ring pattern in $BaTiO_3$ films grown on Pt electrodes is indicative of biaxial texture with in-plane texture and corresponds to the (101) and (001) textures compared with a continuous ring pattern in the $BaTiO_3$ film grown on LSCO/Pt electrode.

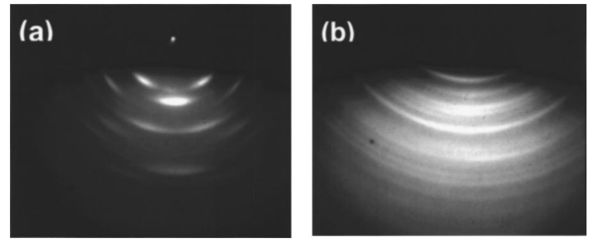

FIG. 2. (Color online) RHEED patterns of $BaTiO_3$ films grown on (a) Pt and (b) LSCO/Pt electrodes.

Figure 3 shows AFM images of the surface morphology of $BaTiO_3$ films grown on Pt and LSCO/Pt electrodes and simultaneously obtained IPP- and OPP-PFM images, respectively. As shown in Figs. 3(a) and 3(b), the surface morphology is represented by a granular-shaped surface with average grain sizes of about 125 and 167 nm for $BaTiO_3$ grown on Pt and on LSCO/Pt, respectively. The rms roughness (standard deviation from the average height of the surface) on $2 \times 2\ \mu m^2$ area was 8.4 and 7.7 nm on $BaTiO_3/Pt$ and $BaTiO_3/LSCO/Pt$ structures, respectively.

The OPP- and IPP-PFM images in Figs. 3(c)–3(f) show grain size-dependent domain distributions. In PFM measurements, ac electric fields are applied along the (001) direction between a bottom electrode and the AFM tip. If non-(001) oriented components in the $BaTiO_3$ thin films exist, the OPP signal will decrease whereas the IPP signal will increase. Most ferroelectric thin films are deposited on substrates with smaller thermal expansion coefficients than that of the ferro-

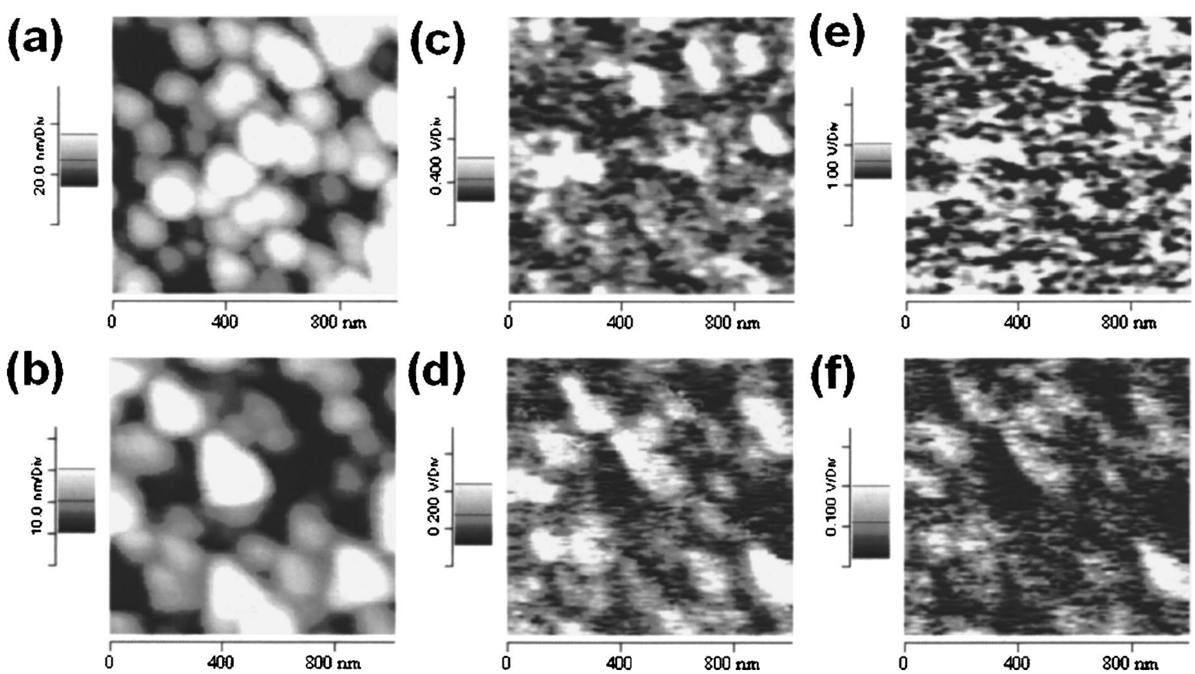

FIG. 3. (Color online) AFM images of surface morphology for (a) $BaTiO_3/Pt$ and (b) $BaTiO_3/LSCO/Pt$, and PFM images of (c) OPP-$BaTiO_3/Pt$, (d) OPP-$BaTiO_3/LSCO/Pt$, (e) IPP-$BaTiO_3/Pt$, and (f) IPP-$BaTiO_3/LSCO/Pt$.

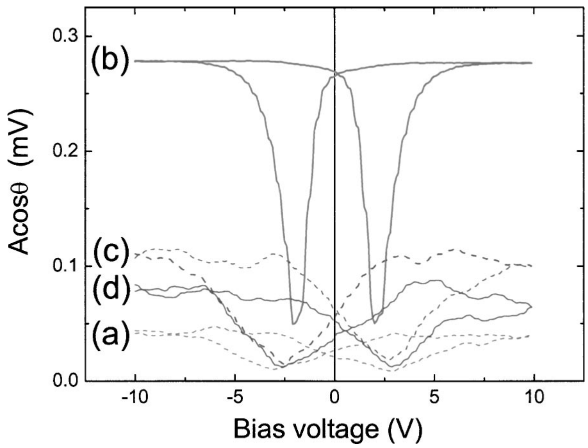

FIG. 4. (Color online) Local piezoresponse hysteresis loops for IPP and OPP components of the $BaTiO_3$ films grown on the Pt and LSCO/Pt electrodes. Effective d_{33} value is obtained from a slope of the linear region in the butterfly loop. (a) OPP signal from $BaTiO_3$/Pt, (b) IPP signal from $BaTiO_3$/Pt, (c) OPP signal from $BaTiO_3$/LSCO, and (d) IPP signal from $BaTiO_3$/LSCO.

electric thin film itself. In-plane stress may develop in the film upon cooling after deposition. This leads to an increase of the in-plane polarization component and is one of the main reasons why thin films have weak spontaneous polarization along direction normal to the film surface. It is believed that the (101) component in $BaTiO_3$/Pt film causes an increase in the in-plane component which increases the IPP signal. The dielectric properties of $BaTiO_3$ films were characterized through the investigation of capacitors with Pt/$BaTiO_3$/Pt and Pt/$BaTiO_3$/LSCO/Pt configurations (not shown). The results showed that $BaTiO_3$ films grown on LSCO/Pt had a higher dielectric constant ($\varepsilon \sim 1000$) than that of $BaTiO_3$ films grown on Pt electrode ($\varepsilon = 570$). It may be inferred from this observation that $BaTiO_3$ films grown on LSCO/Pt have a larger grain size and (001) orientation component compared to that of $BaTiO_3$ films grown on Pt as shown in Figs. 1 and 3. This result is similar to the dielectric behavior of $Ba_{0.5}Sr_{0.5}TiO_3$ (BST) deposited by sputtering on Pt and LSCO/Pt electrodes. $Ba_{0.5}Sr_{0.5}TiO_3$ (BST) films with highly (100) preferred orientation on LSCO/Pt showed smother surface roughness, higher dielectric constant, and improved tunability compared to BST films on Pt with (110) preferred orientation.[11]

Figure 4 shows local piezoreponse hysteresis loops of $BaTiO_3$ films grown on Pt and LSCO/Pt electrodes. Local $P-E$ curves in each measurement show typical butterfly-like shape due to the electric field-induced strain under the AFM tip. The piezoresponse hysteresis loop was recorded as an $A \cos \theta$ signal. Here, A is the amplitude of the first harmonic signal, which provides information on the magnitude of the piezoelectric coefficient (d_{33}) in the measured z direction and θ is the phase shift between the ac voltage signal applied on the AFM tip and the piezoelectric response which determines the direction of polarization. The $A \cos \theta$ relates to the ac field-induced strain according to the equation: $A \cos \theta = -(\partial C/\partial z/k_{\mathrm{lever}})(V_{\mathrm{dc}}-V_c)V_{\mathrm{ac}} \pm d_{33}V_{\mathrm{ac}}$. The symmetry of the curve depends on the 180° domain wall behavior, film residual stress, or effective domain clamping of some domains in preferential orientations. As shown in Fig. 4, The $BaTiO_3$ films grown on the Pt electrode have higher IPP and lower OPP signals. These are consistent with the XRD result in which $BaTiO_3$ grown on a Pt electrode had a (101) preferred orientation with very small (001) peak intensity. The transverse piezoelectric coefficient (large d_{15} of 400 pm/V and negative d_{31} of −35 pm/V) was higher than the longitudinal coefficient (d_{33}=85 pm/V). From the slope of the piezoelectric strain curve, effective d_{33} values are obtained. The measured effective d_{33} values of $BaTiO_3$ films deposited on Pt and LSCO/Pt electrodes were 14.3 and 54.0 pm/V, respectively. Smaller effective d_{33} values than that obtained for single crystals is mainly due to the effect of substrate constraint, grain size, defects, and orientation. In this study, these smaller d_{33} values result from stresses induced by substrate clamping and relevant orientation effects. The impact of substrate clamping on properties was demonstrated by Roytburd *et al.*, who used focused ion beam to relieve the substrate constraint and diminish the internal stresses on a ferroelectric thin film.[12]

In conclusion, the effects of crystal orientation on the piezoelectric properties of $BaTiO_3$ thin films grown on Pt and LSCO/Pt electrodes have been investigated. Thin films deposited on Pt exhibit strong (101) orientation whereas films deposited on LSCO electrodes show mixed (001) and (101) orientations. The abnormal increase of the IPP signal in $BaTiO_3$ grown on Pt is closely related to the preferred (101) orientation of the polycrystalline $BaTiO_3$ films. The measured effective d_{33} values of $BaTiO_3$ films deposited on Pt and LSCO/Pt electrodes were 14.3 and 54.0 pm/V, respectively. Ferroelectric domains are thought to be clamped and stressed by the planar and biaxial stress exerted by the substrate and film lattice mismatch.

This work has been supported by the Army Research Office (ARO-MURI) under Grant No. DAAD 19-01-1-0517, and Arrowhead Research Corporation.

[1] L. E. Cross, *Ferroelectric Ceramics*, edited by N. Setter (Birkhauser Basel, 1993).
[2] Y. B. Park, J. L. Ruglovsky, and H. A. Atwater, Appl. Phys. Lett. **85**, 455 (2004).
[3] F. Felten, G. A. Schneider, J. M. Sladana, and S. V. Kalinin, J. Appl. Phys. **96**, 563 (2004).
[4] A. Petraru, J. Schubert, M. Schmid, O. Trithaveesak, and Ch. Buchal, Opt. Lett. **28**, 2527 (2003).
[5] P. Tang, D. J. Towner, A. L. Meier, and B. W. Wessel, Electron. Lett. **39**, 23 (2003).
[6] S. E. Park, S. Wada, L. E. Cross, and T. R. Shrout, J. Appl. Phys. **86**, 2746 (1999).
[7] N. Stavistki, V. Lyahovitskaya, J. Nair, I. Zon, R. Popovitz-Biro, E. Wachtel, Y. Feldman, and I. Lubomirsky, Appl. Phys. Lett. **81**, 4177 (2000).
[8] O. Auciello, A. Gruverman, H. Tokumoto, S. A. Prakash, S. Aggarwal, and R. Ramesh, MRS Bull. 33 (1998).
[9] H. R. Zeng, H. F. Yu, R. Q. Chu, G. R. Li, H. S. Luo, and Q. R. Yin, J. Cryst. Growth **267**, 194 (2004).
[10] S. V. Kalinin and D. A. Bonnell, Phys. Rev. B **65**, 125408 (2002); S. V. Kalinin, A. Gruverman, and D. A. Bonnell, Appl. Phys. Lett. **85**, 795 (2004).
[11] I. D. Kim, J. H. Park, and H. G. Kim, Electrochem. Solid-State Lett. **5**, F18 (2002).
[12] A. L. Roytburd, S. P. Alpay, V. Nagarajan, C. S. Ganpule, S. Aggarwal, E. D. Williams, and R. Ramesh, Phys. Rev. Lett. **85**, 190 (2000).